

AD-A144 174

INVESTIGATION OF RAPIDLY SOLIDIFIED NI3AL-BASED ALLOYS  
(U) GENERAL ELECTRIC CORPORATE RESEARCH AND DEVELOPMENT  
SCHENECTADY NY S C HUANG ET AL. 31 MAY 84 84SRD034

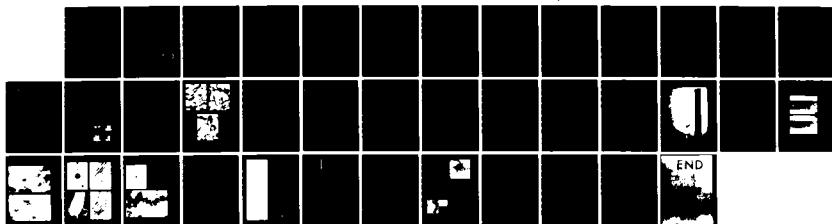
1/1

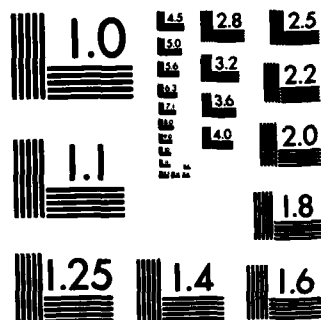
UNCLASSIFIED

N00014-83-C-0199

F/G 11/6

NL





12

AD-A144 174

# INVESTIGATION OF RAPIDLY SOLIDIFIED Ni<sub>3</sub>Al-BASED ALLOYS

Final Report  
Contract No. N00014-83-C-0199

Prepared for

Department of the Navy  
Office of Naval Research  
Arlington, Virginia 22217

Prepared by

Alloy Properties Branch  
Metallurgy Laboratory  
Corporate Research and Development  
General Electric Company  
Schenectady, New York 12301

May 1984

DTIC  
ELECTE  
AUG 8 1984  
B

Reproduction in whole or in part is permitted for any  
purpose of the United States Government

Approved for public release: distribution unlimited

84 08 06 124

DTIC FILE COPY

unclassified

SECURITY CLASSIFICATION OF THIS PAGE

AD-A122 174

# REPORT DOCUMENTATION PAGE

1a. REPORT SECURITY CLASSIFICATION unclassified		1b. RESTRICTIVE MARKINGS	
2a. SECURITY CLASSIFICATION AUTHORITY		3. DISTRIBUTION/AVAILABILITY OF REPORT Approved for public release; distribution unlimited	
2b. DECLASSIFICATION/DOWNGRADING SCHEDULE			
4. PERFORMING ORGANIZATION REPORT NUMBER(S) 84SRD034 ✓		5. MONITORING ORGANIZATION REPORT NUMBER(S)	
6a. NAME OF PERFORMING ORGANIZATION General Electric Company Corporate Research and Development	6b. OFFICE SYMBOL (If applicable)	7a. NAME OF MONITORING ORGANIZATION	
6c. ADDRESS (City, State and ZIP Code) Schenectady, NY 12301		7b. ADDRESS (City, State and ZIP Code)	
8a. NAME OF FUNDING/SPONSORING ORGANIZATION Department of the Navy Office of Naval Research	8b. OFFICE SYMBOL (If applicable) Code 430	9. PROCUREMENT INSTRUMENT IDENTIFICATION NUMBER N00014-83-C-0199	
8c. ADDRESS (City, State and ZIP Code) Arlington, VA 22217		10. SOURCE OF FUNDING NOS.	
11. TITLE (Include Security Classification) Investigation of Rapidly Solidified Ni <sub>3</sub> Al-Based Alloys		PROGRAM ELEMENT NO.	PROJECT NO.
		TASK NO.	WORK UNIT NO.
12. PERSONAL AUTHOR(S) S.C. Huang, K.M. Chang, A.I. Taub			
13a. TYPE OF REPORT Final Report	13b. TIME COVERED FROM 1 Mar 1983 TO 29 Feb 1984	14. DATE OF REPORT (Yr., Mo., Day) 31 May 1984	15. PAGE COUNT 50
16. SUPPLEMENTARY NOTATION			
17. COSATI CODES		18. SUBJECT TERMS (Continue on reverse if necessary and identify by block number)	
FIELD	GROUP	SUB. GR.	
		rapid solidification, intermetallic compounds, nickel-aluminide	
19. ABSTRACT (Continue on reverse if necessary and identify by block number)			
<p>The addition of one atom percent boron to Ni<sub>3</sub>Al makes this otherwise-brittle alloy ductile. Rapid solidification also makes it strong. The effects of boron concentration, Ni:Al stoichiometry, and quaternary element additions were studied and are reported.</p>			
20. DISTRIBUTION/AVAILABILITY OF ABSTRACT UNCLASSIFIED/UNLIMITED <input type="checkbox"/> SAME AS RPT. <input checked="" type="checkbox"/> DTIC USERS <input type="checkbox"/>		21. ABSTRACT SECURITY CLASSIFICATION unclassified	
22a. NAME OF RESPONSIBLE INDIVIDUAL Dr. Donald E. Polk		22b. TELEPHONE NUMBER (Include Area Code) 202-696-4402	22c. OFFICE SYMBOL Code 430

## TABLE OF CONTENTS

Section	Page
1 INTRODUCTION .....	1-1
1.1 Background .....	1-1
1.2 Precontract Work .....	1-1
2 CONTRACT PROGRESS .....	2-1
2.1 Effects of Boron Concentration .....	2-1
2.2 Quaternary Alloying Behaviors .....	2-2
2.3 Importance of Stoichiometry .....	2-4
2.4 Effect of Cobalt on Ductility .....	2-4
2.5 Elevated Temperature Mechanical Properties .....	2-4
3 REFERENCES .....	3-1
Appendix A .....	A-1
Appendix B .....	B-1
Appendix C .....	C-1

Accession For	
NTIS GRA&I	<input checked="" type="checkbox"/>
DTIC TAB	<input type="checkbox"/>
Unannounced	<input type="checkbox"/>
Justification	
By _____	
Distribution/	
Availability Codes	
Dist	Avail and/or Special
A-1	



## Section 1

### INTRODUCTION

#### 1.1 Background

The intermetallic compound  $\text{Ni}_3\text{Al}$  exhibits great strength in the temperature range from 600 to 900 °C. In addition, the lightweight aluminide—although not containing the strategic element chromium—is extremely resistant to oxidation. The actual application of  $\text{Ni}_3\text{Al}$  as a high-temperature material, however, has not been realized because of its poor low-temperature properties. At room temperature, polycrystalline  $\text{Ni}_3\text{Al}$  fractures at a stress less than 30 ksi, with essentially no ductility.<sup>(1)</sup>

After extensive research over the last 25 years,<sup>(1-3)</sup> it only recently has been found that the low-temperature ductility of the polycrystalline  $\text{Ni}_3\text{Al}$  can be improved significantly by the addition of the ternary element boron.<sup>(4)</sup> Although the beneficial effect of boron is not yet understood, this discovery has been confirmed by researchers at the Oak Ridge National Laboratory. The boron-modified  $\text{Ni}_3\text{Al}$  remains weak, however, with no improvement in low-temperature strength.

#### 1.2 Precontract Work

Remarkable increases in the room-temperature strength of the boron-modified  $\text{Ni}_3\text{Al}$  have been achieved in the Metallurgy Laboratory of General Electric Corporate Research and Development through the rapid-solidification, melt-spinning process. Specifically, it has been shown that a ribbon of  $\text{Ni}_3\text{Al}$ -1.0 at% B has a yield stress of 100 ksi, which represents a threefold improvement. Furthermore, the ductility imparted by the boron addition has been maintained in the rapidly solidified ribbons.

## Section 2

### CONTRACT PROGRESS

The beneficial effects of boron and rapid solidification on the strength and ductility of  $\text{Ni}_3\text{Al}$  were investigated under contract N00014-83-C-0199. The extent to which the rapid-solidification-induced improvements can withstand heat treatment was also evaluated, and the effects of quaternary element additions on boride formation and solid solution strengthening were studied. Details of the results follow.

#### 2.1 Effects of Boron Concentration

The solution behavior of boron in melt spun  $\text{Ni}_3\text{Al}$  has been characterized.<sup>(5-7)</sup> X-ray diffraction measurements showed that the  $\text{Ni}_3\text{Al}$  lattice parameter increases monotonically with boron additions up to 6.0 at%. It was found that the lattice strain per boron atom fraction is substantially larger than that of the substitutional elements, indicating the interstitial nature of the boron. The lattice parameter results, however, gave no indication of a solution limit within the boron range investigated.

A transmission electron microscopy (TEM) study showed the matrix phase of the ribbons to be of the ordered, face-centered-cubic, L12 type. TEM also confirmed that no boride is formed with  $B \leq 1.5$  at%. The only secondary phase found was a fine, Al-rich, twinned martensitic phase that was observed in the boron-free ribbon, but which was completely suppressed by small additions of boron. However, a dispersion of  $\text{M}_{23}\text{B}_6$  boride was observed in ribbons containing  $B > 1.5$  at%. Compared with the solubility of 0.5 at% boron in slowly cooled  $\text{Ni}_3\text{Al}$ ,<sup>(4)</sup> the present results indicate a boron solution limit that is significantly extended by the rapid solidification technique of melt spinning.

The effect of boron level on the room temperature strength and ductility of rapidly solidified nickel aluminide is shown in Figure 1. The tensile ductility is a strong function of boron concentration, rising steeply from zero ductility, for no boron addition, to about 20% for 0.75 at% boron, and falling precipitously to almost nil ductility at 1.5 at% boron. This variation in the measured ductility is matched by corresponding changes in the fracture morphology. The alloy with no boron addition exhibits pure intergranular failure. The alloys with boron levels  $0.5 \leq x \leq 1.0$  at% exhibit a mixed mode failure containing patches of intergranular failure and regions that appear to be ductile fracture. With  $x > 1.5$  at% boron addition, the fracture mode reverts to intergranular with the appearance of borides on the grain boundaries.

In contrast to the ductility, the yield strength of the nickel aluminide increases monotonically with increasing boron addition. Further, up to the solubility limit of 1.5 at%, the strength varies linearly with boron concentration, with a potency that is at least three times that of any substitutional elements. The linear strength-boron level relationship breaks down beyond the solubility limit of 1.5 at%.

The potency of boron in strengthening nickel aluminide appears to be associated with the large lattice strains that it produces by occupying interstitial lattice positions. Whereas the greater than 200% increase in strength of rapidly solidified boron-free  $\text{Ni}_3\text{Al}$ —as compared to the conventionally cast alloy—is attributed to the quenched-in residual stresses and the refined grain size, our work has shown that the boron

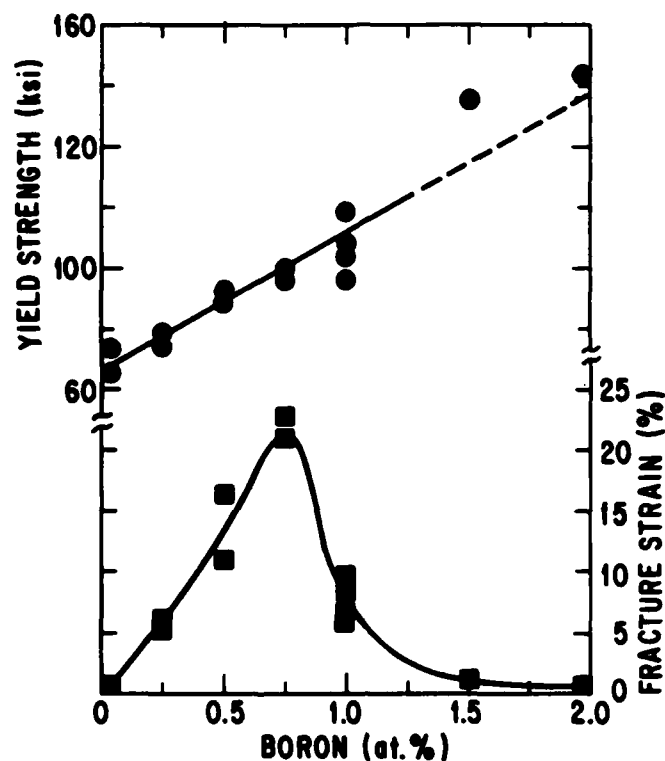


Figure 1. The effect of boron additions on the tensile yield strength and elongation of melt spun  $\text{Ni}_3\text{Al}$  ribbon.

strengthening is not associated with any additional residual stresses or microstructural refinement. Rather, the large amount of strengthening measured for boron in melt spun  $\text{Ni}_3\text{Al}$  is in agreement with the Mott-Nabarro theory of solid solution hardening.<sup>(8)</sup> In this regard, comparison with data on other solid solution elements such as Fe, Ti, Cr, Si and V<sup>(2,9)</sup> shows boron to be a particularly potent strengthener in  $\text{Ni}_3\text{Al}$ .

## 2.2 Quaternary Alloying Behaviors

Based on the above results,  $\text{Ni}_3\text{Al} + 1.0 \text{ at\% B}$  was selected as the base composition into which a variety of quaternary elements were added to investigate the alloying behavior. The resultant ribbon microstructure and bend ductility of the quaternary alloys are listed in Table 1, which shows a correlation of full-bend ductility to the equiaxed microstructure. The equiaxed structure as observed in ribbons containing Co, V, and Si is believed to result from recrystallization that can readily occur in a single-phase material. It appears that Co, V, and Si, at about the 5 at% level, can be kept in solution by the melt spinning process, and thus not form borides or a beta phase.

Two of the ribbons have been further characterized by tensile tests. As seen in the stress-strain curves in Figure 2, the Si-added ribbon exhibits a yield stress as high as  $\sim 170 \text{ ksi}$  with little loss in ductility. On the other hand, the Co addition imparts only a moderate strength improvement, but with a twofold increase in ductility over the base alloy.



**Table 1**  
**QUATERNARY ALLOYS BASED ON  $\text{Ni}_3\text{Al} + 1 \text{ AT\% B}$**

Alloy Number	Composition Formula	Ribbon Bend Ductility	Structure
92	$(\text{Ni}_{0.75}\text{Al}_{0.20}\text{Ti}_{0.05})_{99}\text{B}_1$	0.04	Nonequiaxed (NE)
111	$(\text{Ni}_{0.75}\text{Al}_{0.20}\text{Ta}_{0.05})_{99}\text{B}_1$	0.03	NE
112	$(\text{Ni}_{0.75}\text{Al}_{0.20}\text{Nb}_{0.05})_{99}\text{B}_1$	0.02	NE
113	$(\text{Ni}_{0.75}\text{Al}_{0.20}\text{V}_{0.05})_{99}\text{B}_1$	1.0	Equiaxed (E)
114	$(\text{Ni}_{0.75}\text{Al}_{0.20}\text{Si}_{0.05})_{99}\text{B}_1$	1.0	E
101	$(\text{Ni}_{0.70}\text{Co}_{0.05}\text{Al}_{0.25})_{99}\text{B}_1$	1.0	E
115	$(\text{Ni}_{0.65}\text{Fe}_{0.10}\text{Al}_{0.25})_{99}\text{B}_1$	0.9	NE
116	$(\text{Ni}_{0.65}\text{Mn}_{0.10}\text{Al}_{0.25})_{99}\text{B}_1$	0.04	-
117	$(\text{Ni}_{0.70}\text{Cr}_{0.05}\text{Al}_{0.25})_{99}\text{B}_1$	0.06	NE
125	$[(\text{Ni}_{0.75}\text{Al}_{0.25})\text{Re}_{0.03}]_{99}\text{B}_1$	0.1	-

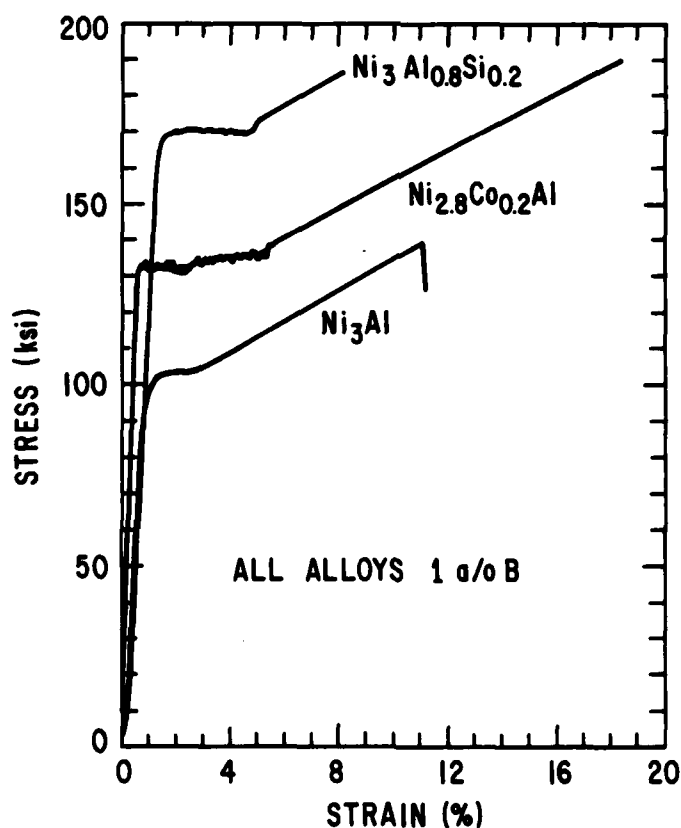


**Figure 2. Tensile behavior of  $\text{Ni}_3\text{Al} + \text{B}$  with additions of Si and Co.**

As shown in Table 1, the addition of Ti, Nb, Ta, Co, Re, Cr, Fe, and Mn leads to nonequiaxed microstructure and embrittled ribbons. A transmission electron microscopy study of the Ti-added ribbon showed a dispersion of  $M_{23}B_6$  boride, which is suspected to be the embrittling phase. It appears that Ti reduces the boron solubility substantially. Two subsequent series of alloys with systematic Ti and B variations show that the Ti embrittling effect exists at all levels of boron, unless Ti is kept  $<2.0$  at%. However, in this series of alloys, one alloy exhibited unexpected full-bend ductility that cannot be accounted for by the Ti or B effects. A chemical analysis of this alloy indicates a (Al + Ti) content of  $\sim 1$  at% less than the nominal 25 at%, which suggests a critical stoichiometry effect on the ductility.

### 2.3 Importance of Stoichiometry

Early data based on stoichiometric  $Ni_3Al$  showed some scatter of both strength and ductility between ribbons produced in different melt spinning runs, even if the runs were from the same ingot. It was found that annealing the ribbons at  $1100^\circ C$  for two hours eliminated the differences found in the as-cast properties of ribbons made from the same starting ingot. Presumably, the scatter in the as-cast properties was due to differences in the residual quenched-in stresses and to subtle differences in microstructure. However, annealing failed to reduce the scatter observed in some of the ribbons produced from different starting ingots. Chemical analysis of the ribbons indicated that variations among ingots in the aluminum-nickel ratio of 24:76. These ribbons consistently showed higher ductilities than the 25:75 aluminum-nickel ribbons, particularly when tested in the annealed condition.

### 2.4 Effect of Cobalt on Ductility

In addition to the stoichiometry effect, the increased ductility by Co additions was demonstrated as described in the quaternary alloy study presented in Section 2.2. This preliminary study was extended to optimize the Co content with regard to the room temperature properties in as-spun and annealed conditions. Again,  $Ni_3Al + 1.0$  at% B was used as the alloy basis, and Co concentrations of 0, 5, 10, 20, and 30 at% substituting for Ni were considered. In the as-cast condition, the yield strength increased with Co concentration, reaching a peak at 20 at% ( $\sim 200$  ksi). The ribbon ductility peaked at a concentration of 5 at% Co. After annealing at  $1100^\circ C$  for two hours, the yield strength was generally reduced and peaked at 10 at% Co (see Figure 3). Note also in Figure 3, that alloys with  $Co \leq 5$  at% lose a substantial portion of their ductility after the anneal. A Co addition of at least 10 at% is necessary to avoid the precipitous drop in the annealed ductility. Based on the annealed ribbon properties of Figure 3, the optimum Co concentration was determined to be 10 at%.

### 2.5 Elevated Temperature Mechanical Properties

Figure 4 shows the elevated temperature yield strength and ductility of the  $Ni_3Al$  with 1 at% boron alloy, in which 10 and 20 at% cobalt additions were substituted for nickel. The data is representative of that found for all the  $Ni_3Al$ -based alloys studied and illustrates several important points. First, the data shown for the 10 at% cobalt alloy are for both ribbon and consolidated powder specimens. This powder work (which is internally funded) is being performed to assess the extent to which the results of ribbon tests can be extrapolated to bulk specimens. The good correlation of properties observed between consolidated powder and ribbon is in agreement with previous work that compared ribbon properties to the properties of material prepared by low-pressure

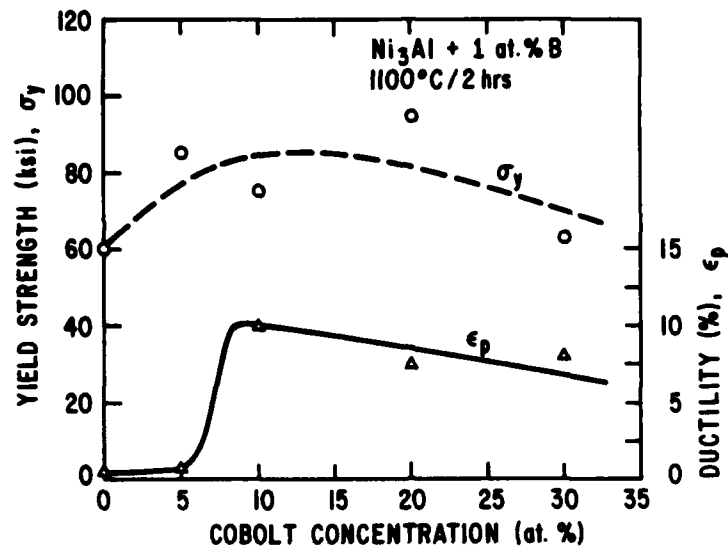


Figure 3. Room temperature tensile properties of annealed  $\text{Ni}_3\text{Al} + \text{B}$  as a function of cobalt content.

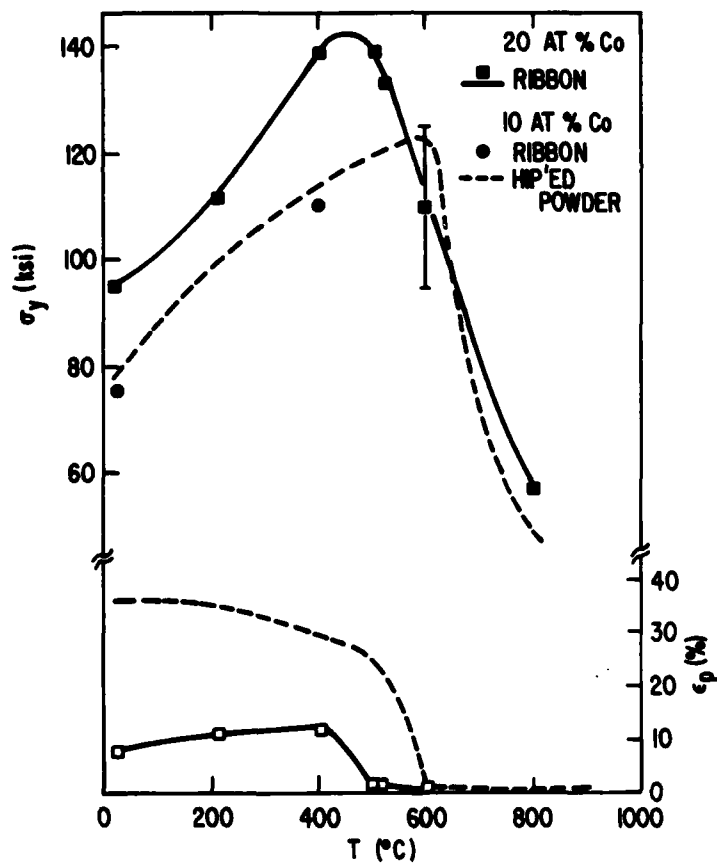


Figure 4. Elevated temperature tensile properties of  $\text{Ni}_3\text{Al} + \text{B} + \text{Co}$  in ribbon form and in consolidated powder form.

plasma deposition.<sup>(10)</sup> The correlation of the ribbon yield strength data with bulk specimens is excellent. The ductility data is a good illustration of our general conclusion that the ductility measured for ribbons is useful as a relative indicator for alloy comparison and temperature effects, but representative only of a minimum value for bulk specimen ductility.

The data also shows that the unusual behavior of the yield strength associated with conventionally cast  $\text{Ni}_3\text{Al}$  (i.e., increasing flow stress with increasing temperature<sup>1</sup>) is retained in the rapidly solidified alloy. Although the ambient temperature strength of the rapidly solidified alloy is considerably greater than that of the conventional casting, the flow stress of the rapidly solidified alloy peaks at about 500-600 °C, compared to about 800 °C for conventionally cast material. Of even greater concern is the severe ductility reduction that occurs in the rapidly solidified alloys from about 500-600 °C to about 800 °C. Examination of the fracture surfaces shows that the failure mode reverts to brittle intergranular fracture in this temperature regime. The cause of this intermediate temperature embrittlement is unclear. Addition of certain quaternary elements has resulted in a shift of the embrittlement onset to higher temperatures, but above that onset temperature, the ductility becomes essentially zero and remains so until the embrittlement temperature range is exceeded.

### Section 3

#### REFERENCES

1. A. Lawley, in *Intermetallic Compounds*, J.H. Westbrook, ed., John Wiley and Sons, (1967) 464.
2. R.W. Guard and J.H. Westbrook, *Trans. AIME* 215, (1959) 807.
3. S. Chakravorty and D.R.F. West, *Met. Tech.*, October 1980, 414.
4. K. Aoki and O. Isumi, *J. Japan Inst. Met.* 43, (1979) 358.
5. A.I. Taub, S.C. Huang and K.M. Chang, *Met. Trans.* 15A (1984) 399.
6. K.M. Chang, S.C. Huang, and A.I. Taub, to be published in *Proc. Symp. Rapidly Solidified Metastable Materials*, The Materials Research Society Meetings, Boston, Nov. 15-17, 1983.
7. S.C. Huang, A.I. Taub, and K.M. Chang, submitted to *Acta Met.*
8. N.F. Mott and F.R.N. Nabarro, in *Report on Conference on the Strength of Solids*, Phys. Soc., London, (1948) 1.
9. R.D. Rawlings and A.E. Staton-Bevan, *J. Mat. Sci.* 10, (1975) 505.
10. A.I. Taub, S.C. Huang, M.R. Jackson, and E.L. Hall, to be published in *Proc. Symp. Rapidly Solidified Metastable Materials*, The Materials Research Society Meetings, Boston, Nov. 15-17, 1983.

**APPENDIX A**

REPRINT 9744

**GENERAL  ELECTRIC**

GENERAL ELECTRIC COMPANY  
CORPORATE RESEARCH AND DEVELOPMENT

P.O. Box 43, Schenectady, N.Y. 12301 U.S.A.

---

**IMPROVED STRENGTH AND DUCTILITY  
OF  $\text{Ni}_3\text{Al}$  BY BORON MODIFICATION  
AND RAPID SOLIDIFICATION**

**A.I. Taub, S.C. Huang, and K.M. Chang**

---

temperatures to (100) at high temperatures. This transition is clearly exhibited in the composition range Fe-45 to -50 at. pct Al. 2. The transition temperature increases with decreasing Al content.

This research was supported in part under Air Force Contract F33615-81-C-5059.

# REFERENCES

1. R. C. Crawford: *Phil. Mag.*, 1976, vol. 33, p. 529.
2. G. Sainfort, P. Montura, P. Peppin, J. Petit, G. Cabane, and M. Salesses: *Memoires Scientifiques Rev. Metallurg.*, 1963, LX2, p. 125.
3. T. Yamagata and H. Yoshida: *Mater. Sci. Eng.*, 1973, vol. 12, p. 95.
4. Y. Umakoshi and M. Yamaguchi: *Phil. Mag. A*, 1980, vol. 41, p. 537.
5. Y. Umakoshi and M. Yamaguchi: *Phil. Mag. A*, 1981, vol. 44, p. 711.
6. T. Yamagata: *Trans. JIM*, 1977, vol. 18, p. 715.
7. A. K. Head, M. H. Loretto, and P. Humble: *Phys. Status Solidi*, 1967, vol. 20, p. 521.
8. I. L. Ray, R. C. Crawford, and D. J. H. Cockayne: *Phil. Mag.*, 1970, vol. 21, p. 1027.

## Improved Strength and Ductility of Ni<sub>3</sub>Al by Boron Modification and Rapid Solidification

A. I. TAUB, S. C. HUANG, and K. M. CHANG

The intermetallic compound Ni<sub>3</sub>Al is unusual in that the flow stress increases with temperature, reaching a peak value at approximately 800 °C.<sup>1,2,3</sup> This behavior would make the compound attractive as a refractory material were it not for the low ductility exhibited by the cast material at ambient temperature. This low ductility of polycrystalline Ni<sub>3</sub>Al has been attributed to the inherent weakness of the grain boundaries, since single crystals of the compound have been shown to exhibit high ductilities in all crystal orientations, even at room temperature.<sup>4</sup> In an attempt to improve the ductility of the polycrystalline form of the compound, Aoki and Izumi<sup>5,6</sup> introduced small additions of boron to the binary intermetallic. The boron addition resulted in a considerable improvement in the ductility, more than 30 pct plastic strain for addition of approximately 0.5 at. pct boron compared to zero ductility for unmodified Ni<sub>3</sub>Al processed under identical conditions. This is consistent with a recent calculation of the effect of boron on the binding strength of a Ni cluster, in which Messmer and Briant<sup>7</sup> showed that the boron acts to enhance the electronic bonding between the Ni atoms. An improvement of the ductility of sulfur doped nickel by boron additions has also been attributed to grain boundary modification.<sup>8</sup>

In this paper, we will report the preliminary results of an investigation into the effect of cooling rate on the me-

chanical properties of the Ni<sub>3</sub>Al intermetallic phase. In particular, the effects of rapid solidification on the strength and ductility of boron modified Ni<sub>3</sub>Al will be discussed.

The ingots of Ni<sub>3</sub>Al with various boron additions were prepared by vacuum induction melting using high purity Ni, Al, and NiB. The ingots were then processed into ribbon form (approximately 6 mm wide by 20 to 35 μm thick) via melt spinning in vacuum. Details of the melt spinning process for Ni based alloys have been presented elsewhere.<sup>9</sup>

The mechanical properties of the ribbons were measured by both bend and tensile tests. In the bend ductility tests, one determines the ability to bend the ribbon 180 deg without fracturing. This test provides a quick measure of the brittleness of the ribbon. We have found that those ribbons that cannot be bent the full 180 deg without fracturing never exhibit any tensile ductility. However, the test cannot measure the relative ductility of those ribbons which can be bent the full 180 deg. On the other hand, the strain to failure of the ribbon as measured in tensile tests can be used to compare the ductilities of different alloys.

The ribbons were tensile tested at both ambient and elevated temperature in a standard Instron static tensile testing machine. The high temperature tests were performed in an argon atmosphere, at a strain rate of  $8.3 \times 10^{-4} \text{ s}^{-1}$ . The room temperature tests were conducted at tensile strain rates of  $1.7 \times 10^{-5} \text{ s}^{-1}$  and  $8.3 \times 10^{-4} \text{ s}^{-1}$ , with no observable differences. The load was converted to stress using the cross-sectional area (A) of the specimen as determined by measuring the weight (W) and length (L) of the specimens:  $A = W/L\rho$ , where  $\rho$  is the density of the alloy. This area determination technique is necessary because of the irregularities in the ribbon geometry.<sup>10</sup>

The effect of boron on the ductility of Ni<sub>3</sub>Al is illustrated in Figure 1 which shows samples of ribbon for each of the compositions as tested for 180 deg bend ductility. The unmodified Ni<sub>3</sub>Al exhibits no ductility. The alloy modified with 2 at. pct boron shows signs of tearing on bending. The

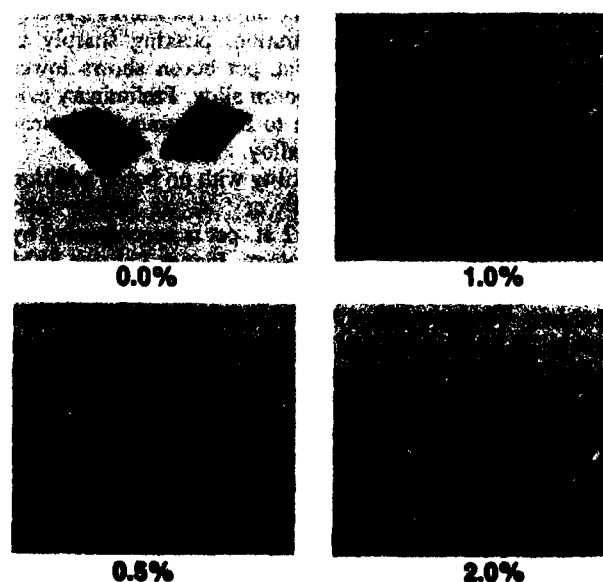


Fig. 1—Ribbons of Ni<sub>3</sub>Al modified with 0.0, 0.5, 1.0, and 2.0 at. pct boron, following 180 deg bend test.

A. I. TAUB, S. C. HUANG, and K. M. CHANG are all Staff Metallurgists with General Electric Corporate Research and Development, P. O. Box 8, Schenectady, NY 12301.

Manuscript submitted August 10, 1983.



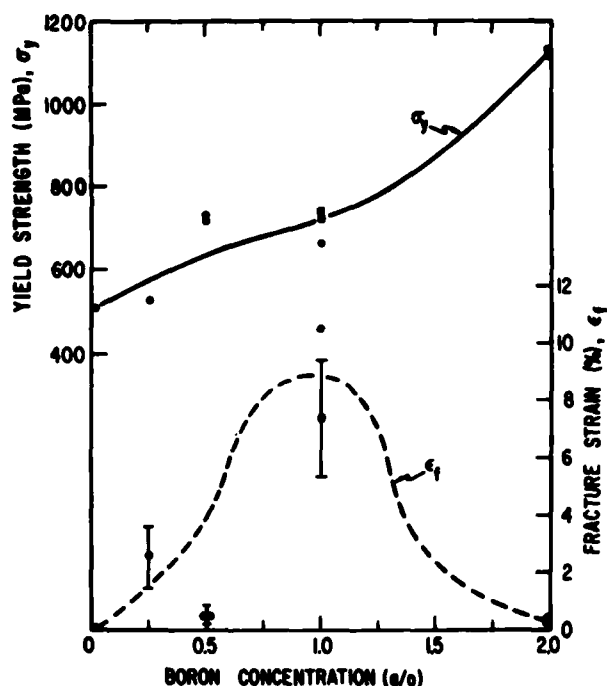


Fig. 2—0.2 pct offset yield strength (open symbols) and strain to failure after yield (closed symbols) of melt spun  $\text{Ni}_3\text{Al}$  modified with the indicated boron levels. The data for a second heat of the 1.0 at. pct boron alloy are shown (squares). The yield strength for the 0.0 boron alloy is actually the highest fracture stress obtained from testing several ribbons, all of which failed in the elastic region.

0.5 and 1.0 at. pct boron modified alloys could be bent to the full 180 deg, with no signs of fracturing.

The tensile test results shown in Figure 2 exhibit the same variation in the ductility with boron level as measured in the bend tests. Further, the increased sensitivity of the tensile tests permits one to distinguish between the degree of ductility of the alloys, particularly those which can be bent fully without fracturing. The ductility exhibits a strong dependence on boron concentration, peaking sharply at 1 at. pct. The alloy with 0.5 at. pct boron shows lower ductility than the 0.25 at. pct boron alloy. Preliminary evidence suggests that this is due to high aluminum content found in the 0.5 at. pct boron alloy.

The transition from zero ductility with no boron addition to approximately 10 pct ductility at 1 at. pct addition and back to nearly zero ductility at 2 at. pct is accompanied by a change in the fracture morphology. Figure 3 shows SEM fractographs of the tensile tested ribbons for the three compositions. The unmodified  $\text{Ni}_3\text{Al}$  exhibits pure intergranular failure. The 1 at. pct boron modified  $\text{Ni}_3\text{Al}$  exhibits a mixed mode failure containing patches of brittle intergranular failure and regions of what appears to be ductile fracture. The specific mechanism of this mixed mode fracture is unclear at this time. With 2 at. pct boron addition, the fracture mode reverts to intergranular with the appearance of borides on the grain boundaries.

Figure 2 shows that the boron additions affect the yield strength of the alloy as well as the ductility. A monotonic increase in strength with boron level is observed. In Figure 4, preliminary results on the elevated temperature

strength of the 1 at. pct boron alloy are shown. Also shown in the figure are the yield strengths of both boron modified and unmodified  $\text{Ni}_3\text{Al}$  processed without rapid solidification. For the same degree of boron addition, the rapidly solidified alloy exhibits a much higher strength. Further, up to 400 °C the strength is observed to increase with temperature in the same manner as the alloys prepared without rapid solidification. In tensile tests above 400 °C, the ribbons appear to embrittle severely, and the specimens break during elastic loading. This premature failure precludes the determination of a yield strength above 400 °C. The embrittlement is limited to the high temperature regime and does not represent a change in the alloy microstructure or composition, as demonstrated by the high ductilities exhibited during room temperature retesting of the high temperature tested specimens. Further investigation into this phenomenon is continuing.

One means of accounting for the increased yield stress of the rapidly solidified alloy may be the fine grain size (5 to 10  $\mu\text{m}$ ). Early work by Grala<sup>11</sup> on cast  $\text{Ni}_3\text{Al}$  showed that coarser microstructures produced by either slower cooling during the casting or by subsequent homogenizing heat treatment exhibited decidedly lower tensile strengths but ambiguous yield strength variations. However, studies on other intermetallics have shown that a Hall-Petch relationship between yield strength and grain size is obeyed.<sup>12</sup> To check for the effect of grain size, ribbons containing 0.0 and 0.5 at. pct boron were annealed at 1060 °C for four hours. This heat treatment produced grains that had grown completely through the thickness of the ribbons (25 to 30  $\mu\text{m}$ ). The yield strengths of these ribbons are listed in Table I and are seen to have dropped considerably from the as-melt spun condition. Also included in the table are the yield strengths for specimens prepared without rapid solidification. These specimens have coarser microstructures. In the case of the 0.5 at. pct boron alloy prepared for this study via vacuum induction melting into a copper chill mold, the grain size is greater than 1 mm. The data show that for both alloys, the yield strengths tend to decrease with increasing grain size. However, the data are too limited to check for Hall-Petch behavior.

It is worth noting that the yield strength for the 0.5 at. pct boron modified alloy is higher than that of the straight  $\text{Ni}_3\text{Al}$ , in both the as-spun and annealed ribbons, even though the grain sizes are similar in both cases. This result differs from the data of Aoki and Izumi<sup>6</sup> who reported no difference in yield strength for the unmodified and 0.25 at. pct boron alloy. The reasons for this discrepancy are unclear at this time.

In conclusion, the application of rapid solidification to the  $\text{Ni}_3\text{Al} + \text{B}$  system has produced ductile, high strength alloys. The ductility and strength are both dependent on the amount of boron addition. The ductility is strongly dependent on boron level, peaking sharply at 1 at. pct. The yield strength is found to increase monotonically with boron addition.

The yield strength of the rapidly solidified alloy in the melt spun condition is considerably higher than that of the same alloy produced without rapid solidification. This increased strength cannot be explained in terms of grain size alone. Further microstructural characterization is required to understand this phenomenon.



(a)



(b)



(c)

Fig. 3 SEM fractographs of the boron modified Ni-Al ribbons tensile tested at room temperature: (a) 0.0 boron addition exhibits pure intergranular failure; (b) 1.0 boron addition shows mixed mode fracture; (c) 2.0 boron addition exhibits pure intergranular failure with borders on the grain boundaries.

Table I. 0.2 Offset Yield Strength of Boron Modified Ni<sub>3</sub>Al

B Addition At. Pct	Preparation Technique	Heat Treatment	Yield Strength		Grain Size ( $\mu$ m)
			(MPa)	(ksi)	
0.0	melt spinning	none	510+	74+	5 to 10
	melt spinning	1060C/4 hours	195	28	25 to 30
	arc melt [6]	1027C/50 hours	200	29	200
	zone melt [3]	none	160	23	NA
	single crystal [4] (001)	1050C/74 hours	210	30	NA
	(111)		500	73	NA
0.5	melt spinning	none	725	105	5 to 10
	melt spinning	1060C/4 hours	450	65	25 to 30
	induction melt				
	-copper mold	1275C/4 hours	350	51	>1000
	arc melt [6]	1027C/50 hours	200	29	100

+ maximum stress since broke in elastic region  
NA — not applicable

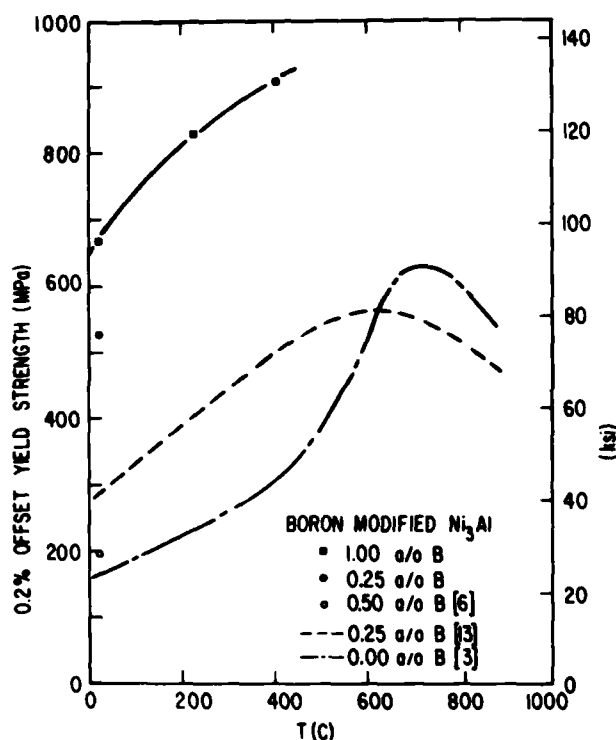


Fig. 4—0.2 pct offset yield strength plotted against testing temperature for Ni<sub>3</sub>Al modified with the indicated boron additions. The reported data for the same alloy processed without rapid solidification are included for comparison.

#### Note in Proof

Since the writing of this paper, C. C. Koch, *et al.*<sup>14</sup> have reported data on the effects of rapid solidification on Ni<sub>3</sub>Al, using foils prepared by the arc-hammer process. In agreement with our data, they found that with additions of 0.25

and 0.50 at. pct boron, the foils exhibit 180 deg bend ductility, whereas the unmodified Ni<sub>3</sub>Al foils are brittle.

The authors would like to thank R. J. Zabala and R. P. Laforce for producing the ribbons and C. P. Palmer for performing the tensile tests. They also thank the Office of Naval Research for partial support of the work.

#### REFERENCES

1. R. W. Guard and J. H. Westbrook: *Trans. TMS-AIME*, 1959, vol. 215, pp. 807-14.
2. O. Noguchi, Y. Oya, and T. Suzuki: *Metall. Trans. A*, 1981, vol. 12A, pp. 1647-53.
3. P. H. Thornton, R. G. Davies, and T. L. Johnston: *Metall. Trans.*, 1970, vol. 1, pp. 207-18.
4. K. Aoki and O. Izumi: *J. Mat. Sci.*, 1979, vol. 14, pp. 1800-46.
5. K. Aoki and O. Izumi: *Kinzoku*, 1979, vol. 49, pp. 38-41.
6. K. Aoki and O. Izumi: *J. Japan Inst. Met.*, 1979, vol. 43, pp. 1190-96.
7. R. P. Messmer and C. L. Briant: *Acta Metall.*, 1982, vol. 30, pp. 457-68.
8. R. A. Mulford: "Embrittlement of Structural Alloys", *Treatise on Materials Science and Technology*, C. L. Briant and S. Banerji, eds., Academic Press, New York, NY, 1983, vol. 25, pp. 1-19.
9. S. C. Huang and A. M. Ritter: *Proc. AIME Symposium Chemistry and Physics of Rapidly Solidified Materials*, St. Louis, MO, October 26-27, 1982, B. J. Berkowitz and R. O. Scattergood, eds., TMS-AIME, Warrendale, PA, 1983, pp. 25-34.
10. A. I. Taub and J. L. Walter: *Mat. Sci. Eng.*, in press.
11. E. M. Grala: *Mechanical Properties of Intermetallic Compounds*, J. H. Westbrook, ed., John Wiley and Sons, New York, NY, 1960, pp. 358-404.
12. A. Lawley: *Intermetallic Compounds*, J. H. Westbrook, ed., John Wiley and Sons, New York, NY, 1967, pp. 464-90.
13. C. T. Liu and C. C. Koch: "Technical Aspects of Critical Materials Use by the Steel Industry, Vol. IIB", National Bureau of Standards, NBSIR 83-2679-2, 1983, pp. 42-1 to 42-19; also editor's note in *Iron Age*, September 24, 1982, p. 63.
14. C. C. Koch, J. A. Horton, C. T. Liu, O. B. Cavin, and J. O. Scarbrough: *Rapid Solidification Processing, Principles and Technologies III*, R. Mehrabian, ed., National Bureau of Standards, 1983, pp. 264-69.

**APPENDIX B**

Submitted to MRS Symposia Proceeding: "Rapidly Solidified Metastable Materials", November 1983, Boston, MA

**A MICROSTRUCTURE INVESTIGATION  
ON RAPIDLY SOLIDIFIED  $\text{Ni}_3\text{Al}$  CONTAINING BORON**

**K.M.CHANG, S.C.HUANG, AND A.I.TAUB**  
General Electric Corporate Research and Development  
P.O. Box 8, Schenectady, NY 12301

**ABSTRACT**

A small amount of boron addition in rapidly solidified  $\text{Ni}_3\text{Al}$  has been found to yield remarkable improvements in both room-temperature strength and ductility. In this study, the microstructure of melt-spun  $\text{Ni}_3\text{Al}$  ribbons with various boron modifications ranging from 0 to 6.0 at% was investigated in detail by using transmission electron microscopy. All alloy compositions studied reveal a completely ordered fcc  $\text{L1}_2$  matrix phase, in which polygonized dislocation networks and subgrain boundaries are observed. The boron-free  $\text{Ni}_3\text{Al}$  contains a dispersion of an Al-rich martensitic phase consisting of alternate twins. The boron addition tends to suppress the formation of the martensitic phase, but excessive boron ( $\geq 2.0$  at%) causes the precipitation of  $\text{M}_{23}\text{B}_6$  type borides.

## A MICROSTRUCTURE INVESTIGATION ON RAPIDLY SOLIDIFIED $\text{Ni}_3\text{Al}$ CONTAINING BORON

K.M.CHANG, S.C.HUANG, AND A.I.TAUB  
General Electric Corporate Research and Development  
P.O. Box 8, Schenectady, NY 12301

### INTRODUCTION

The intermetallic phase  $\text{Ni}_3\text{Al}$  exhibits a positive temperature dependence of strength, reaching a peak value around  $800^\circ\text{C}$  [1]. Polycrystalline  $\text{Ni}_3\text{Al}$  alloys prepared by the conventional casting provide good ductility and oxidation resistance at high temperatures [2,3], but suffer brittle intergranular fracture with zero plastic elongation at low temperatures [4]. Employing the rapid solidification process and the boron alloying addition has been able to produce high strength  $\text{Ni}_3\text{Al}$  alloys with good ductility at room temperature [5].

This paper reports on the microstructure of rapidly solidified  $\text{Ni}_3\text{Al}$  ribbons doped with various amounts of boron. Special attention is given to the relationship between the boron addition level and the microstructural response. Room-temperature properties of ribbons are discussed in light of the results of the present microstructure investigation.

### EXPERIMENTAL

The stoichiometric  $\text{Ni}_3\text{Al}$  composition and its variations containing boron up to 6.0 at% were melted by vacuum induction using high purity Ni, Al, and NiB. The ingots were then remelted and rapidly quenched into ribbon form approximately 6.0 mm wide by 0.030 mm thick via melt spinning in vacuum. Details of the melt spinning process for Ni-base alloys have been presented elsewhere [6].

The mechanical properties of the ribbons were evaluated by both bend and tensile tests. The more complete testing results including ambient and elevated temperature properties of boron-modified  $\text{Ni}_3\text{Al}$  ribbons were given in a separate paper [7].

Transverse sections of ribbon were mounted and polished for metallography. The etching solution of 10 ml  $\text{HNO}_3$  + 40 ml  $\text{HCl}$  + 50 ml  $\text{H}_2\text{O}$  was selected to reveal the grain structure. The transmission electron microscopy samples were prepared directly from the ribbons after carefully polishing both top and wheel-side surfaces. The standard jet-polishing technique was employed with a 20% perchloric acid-methanol solution at  $-50^\circ\text{C}$ .

### RESULTS AND DISCUSSION

The effect of boron addition on the room temperature ductility of  $\text{Ni}_3\text{Al}$  is illustrated by the results of ribbon bend test. (Figure 1) The boron-free  $\text{Ni}_3\text{Al}$  ribbon fractures into two pieces with little ductility. With either 0.5

or 1.0 at% boron modification, the ribbons can sustain the full 180 degree bending without any indication of cracking. When the boron content is added to 2.0 at%, the ribbon shows signs of tearing when fully bent. Further increase in boron addition causes the ribbon to exhibit the brittle fracture again.

Tensile testing of the as-cast ribbons demonstrates that the rapidly solidified  $\text{Ni}_3\text{Al}$  alloys exhibit a substantially high strength at room temperature, more than twice as high as that processed conventionally. Furthermore, the ribbon yield strength increases monotonically with boron addition. The unique behavior of the positive strength-temperature relationship is also observed in these high strength, ductile ribbons. (Figure 2 [2,8])

The grain structure of the ribbon has been examined metallographically on the ribbon transverse section. All ribbons containing up to 2.0 at% boron show a uniform microcrystalline structure without dendritic growth. Equiaxed grains about 5 to 10  $\mu\text{m}$  in diameter are distributed homogeneously through the ribbon thickness. (Figure 3.a) High boron addition (4.0 at% or more) develops fine grains near the wheel side surface followed by cellular crystals as a result of the directional growth. (Figure 3.b) The change in the solidification morphology to cellular growth is associated with the formation of extensive boride precipitates.

Transmission electron microscopy shows that all rapidly solidified alloys have a similar substructure inside matrix grains, but different minor phases exist depending on the boron content. Electron diffraction analysis confirms the common matrix phase to be the  $\text{Ll}_2$  type, ordered fcc crystal structure. No ordering domain or antiphase boundary is observed. Each grain is divided into several subgrains, and the subgrain boundary is composed of dislocation networks. (Figure 4) These quench-induced dislocations have the  $[110]$  type Burgers vector; no stacking fault can be detected.

The boron-free ribbon shows a dispersion of a fine Al-rich martensite phase that consists of alternate twins. (Figure 5) The size, density, and twin spacing of the martensite particles were found to be proportional to the cooling rate. A small amount of boron addition completely suppresses the formation of the martensite phase and results in a single-phase microstructure. However, the ribbon containing 2.0 at% boron starts to form boride precipitates, and the electron diffraction analysis indicates the boride phase to be of the  $\text{M}_{23}\text{B}_6$  crystal structure. (Figure 6)

The mechanical properties of rapidly solidified  $\text{Ni}_3\text{Al}$  alloys with adequate boron modification can be correlated with their microstructure. The observed high strength is attributable to small grain size, dislocation network, and solid-solutioning of boron, which are resulted from the rapid solidification process. On the other hand, the improvement of low temperature ductility is related to the boron effect on the cohesive strength of the grain boundaries [9]. Elimination of the secondary phase may also benefit the ductility.

## SUMMARY

The microstructure of the intermetallic phase  $\text{Ni}_3\text{Al}$  modified with different boron levels and processed by the melt-spinning technique has been characterized. The rapid solidification rate produced a uniform microstructure with fine grain size and polygonized dislocation networks. Appropriate boron content ( $0.0 < B < 2.0$  at%) resulted in a single phase crystal structure and good ductility at room temperature. A martensite phase enriched in Al was found in the unmodified  $\text{Ni}_3\text{Al}$  ribbon, and  $\text{M}_{23}\text{B}_6$  borides was found in ribbons containing high boron ( $\geq 2.0$  at%). The second phases are detrimental to the ribbon ductility.

## ACKNOWLEDGMENTS

The authors would like to thank R.P. Laforce, M.T. Shea, C.P. Palmer, and R.J. Zabala for their technical assistance. This work was partially supported by the Navy Office of Naval Research under the contract of N00014-83-C-0199.

## REFERENCES

- [1] R.W. Guard and J.H. Westbrook, Trans. TMS-AIME, 215, 807 (1959).
- [2] P.H. Thornton, R.G. Davies, and T.L. Johnston, Met. Trans., 1, 207 (1970).
- [3] R.D. Rawlings and A.E. Staton-Bevan, J. Mater. Sci., 10, 505 (1975).
- [4] K. Aoki and O. Izumi, Trans. JIM, 19, 203 (1978).
- [5] S.C. Huang, K.M. Chang, and A.I. Taub, Rapidly Solidified  $\text{Ni}_3\text{Al}$  Containing Boron, presented at 1983 TMS-AIME Fall Meeting, Philadelphia, PA, Oct. 1983.
- [6] S.C. Huang and K.M. Chang, J. Mater. Sci., in press.
- [7] A.I. Taub, S.C. Huang, and K.M. Chang, Met. Trans., in press.
- [8] C.T. Lia and C.C. Koch in: Technical Aspects of Critical Materials Used by the Steel Industry, Vol.IIB (Center for Materials Science, NBS, June 1983) pp. P42-1.
- [9] R.P. Messmer and C.L. Briant, Acta Met., 30, 457 (1982).



# FIGURE CAPTIONS

- Figure 1.  $\text{Ni}_3\text{Al}$  ribbons modified with 0.0, 0.5, 1.0, and 2.0 at% boron after 180 degree bending test.
- Figure 2. Yield strength as a function of testing temperature of boron-modified  $\text{Ni}_3\text{Al}$  alloys through conventional and rapidly solidified processes [2,8].
- Figure 3. Grain structures of  $\text{Ni}_3\text{Al}$  ribbons containing (a)  $\leq 2.0$  at%, (b)  $\geq 4.0$  at% boron.
- Figure 4. General substructure consisting of subgrains and dislocation networks in melt-spun  $\text{Ni}_3\text{Al} + 1.0$  at% B ribbons.
- Figure 5. Al-rich matensite phase consisting of alternate twins in the boron-free ribbon.
- Figure 6.  $\text{M}_{23}\text{B}_6$  boride precipitates developed in the ribbon containing 4.0 at% boron.

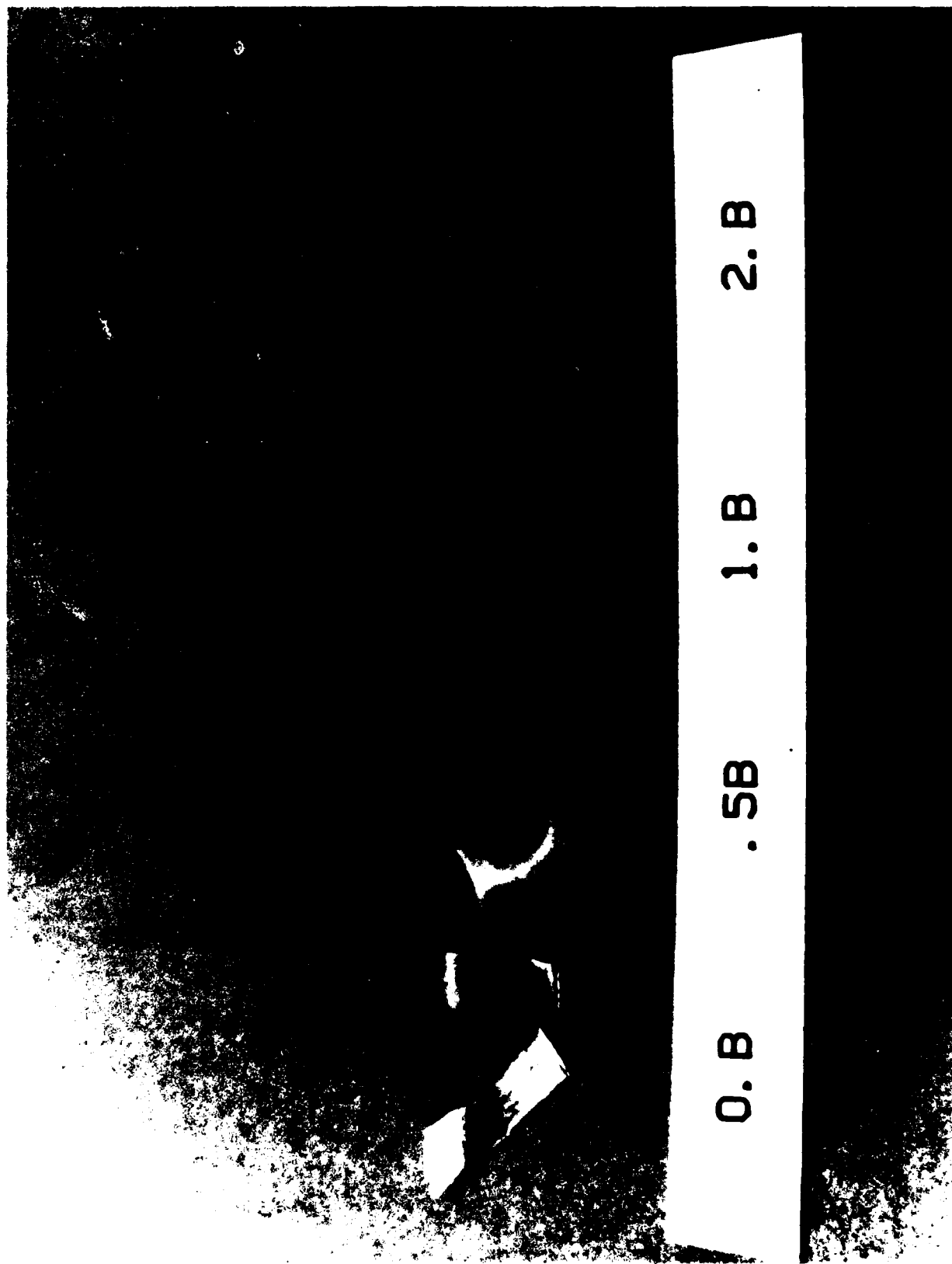


Figure 1.  $\text{Ni}_3\text{Al}$  ribbons modified with 0.0, 0.5, 1.0, and 2.0 at% boron after  $180^\circ$  bending test.

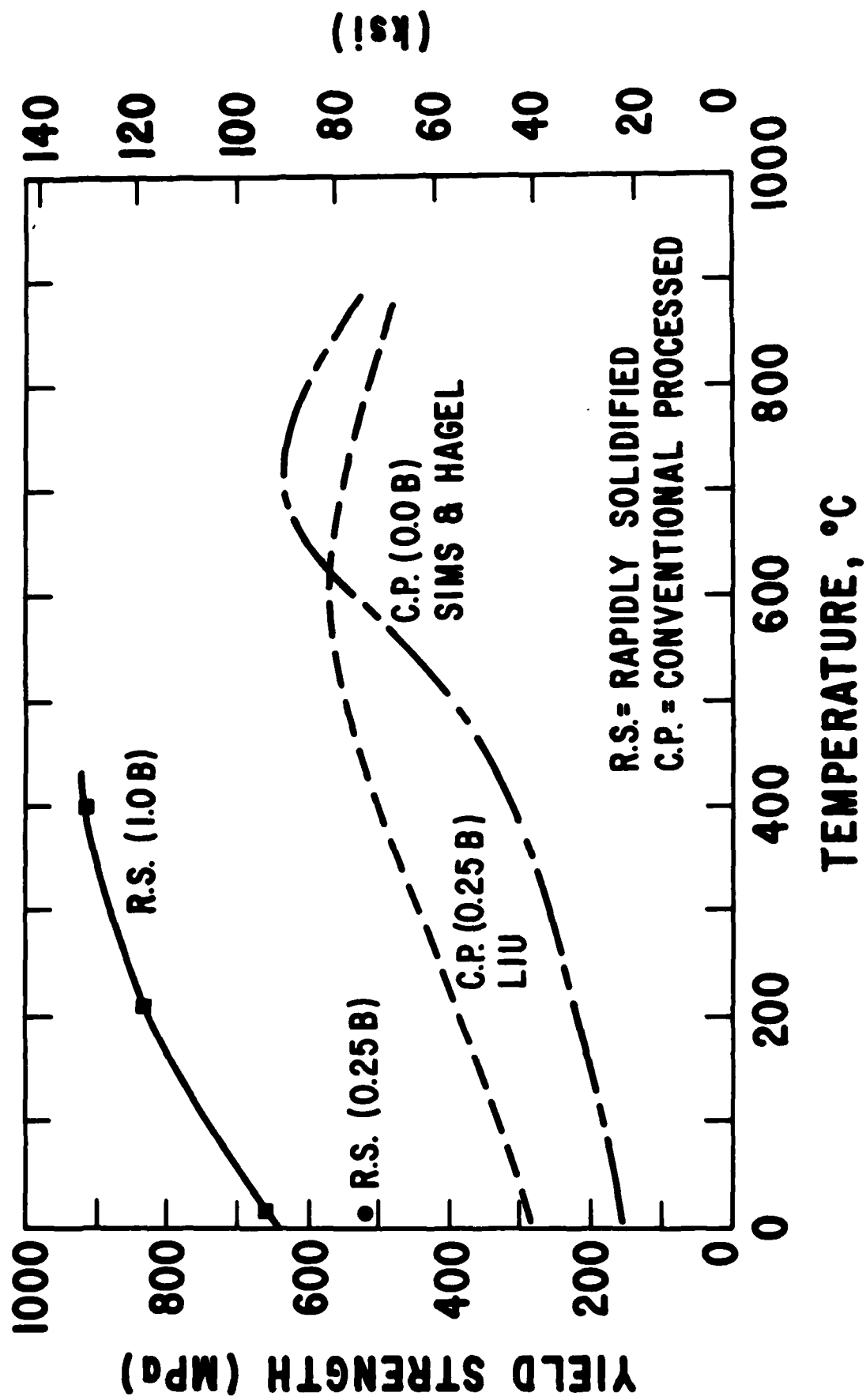


Figure 2. Yield strength as a function of testing temperature of boron-modified  $\text{Ni}_3\text{Al}$  alloys through conventional and rapidly solidified processes [2,8].

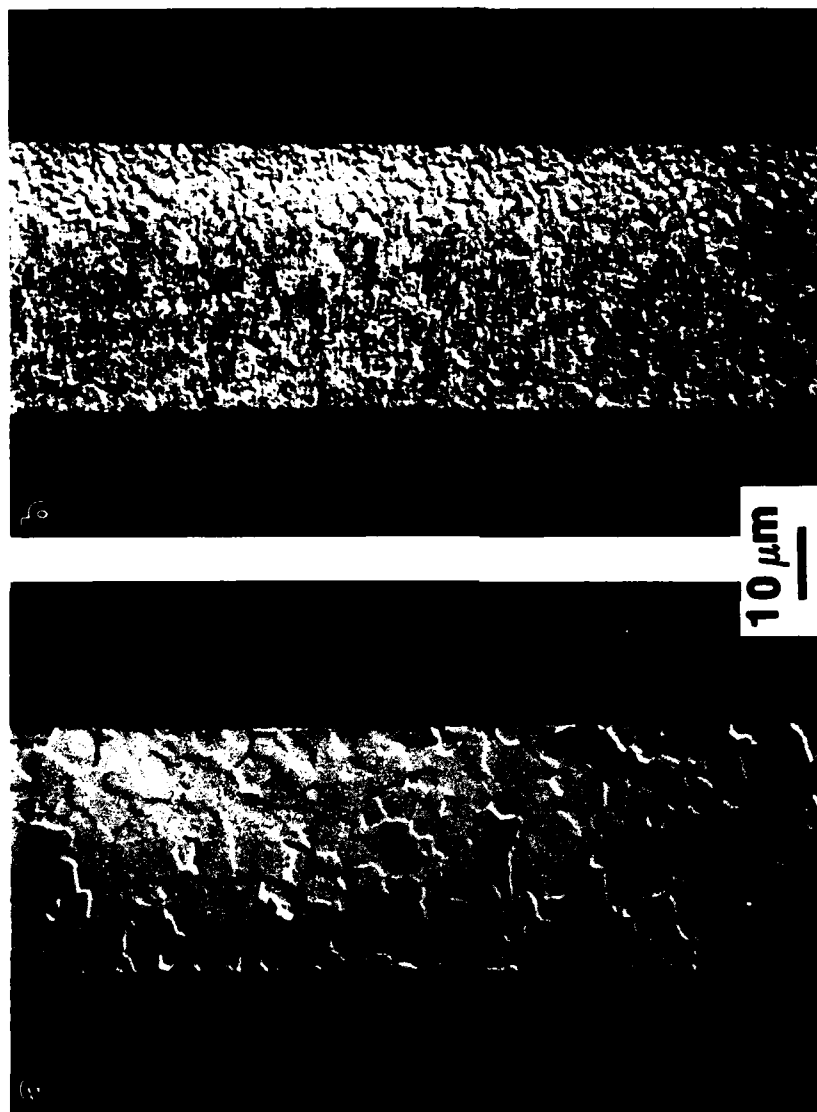


Figure 3. Grain structures of  $\text{Ni}_3\text{Al}$  containing (a)  $\leq 2.0$  at%, (b)  $\geq 4.0$  at% boron.

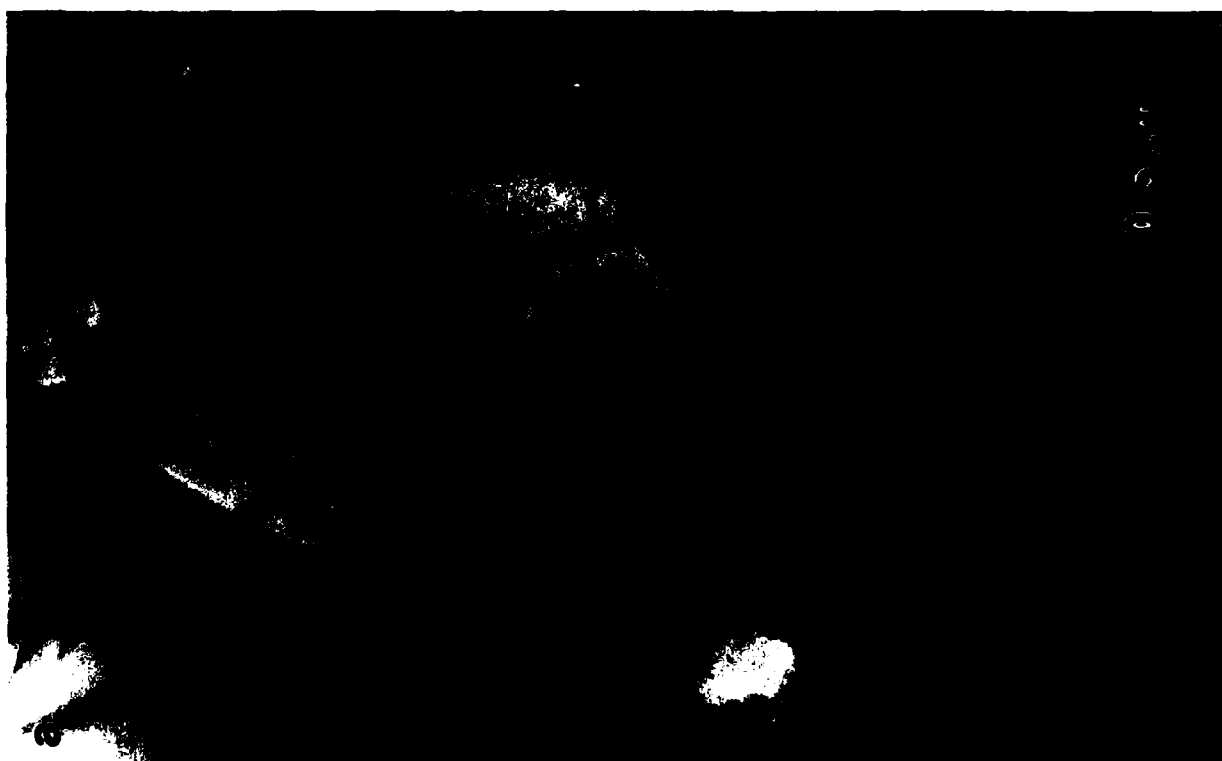


Figure 4. General substructure consisting of subgrains and dislocation networks in melt-spun  $\text{Ni}_3\text{Al} + 1.0 \text{ at\% B}$  ribbons.

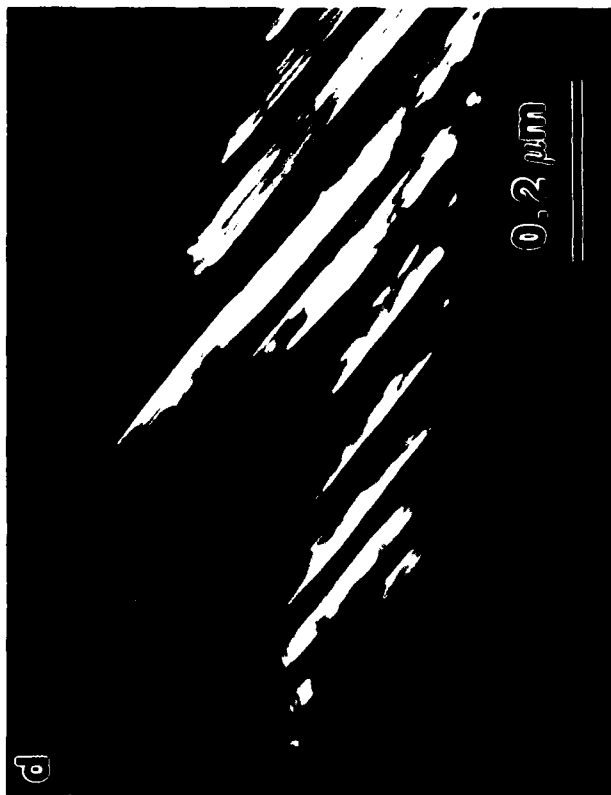
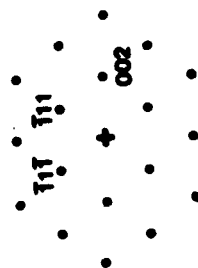
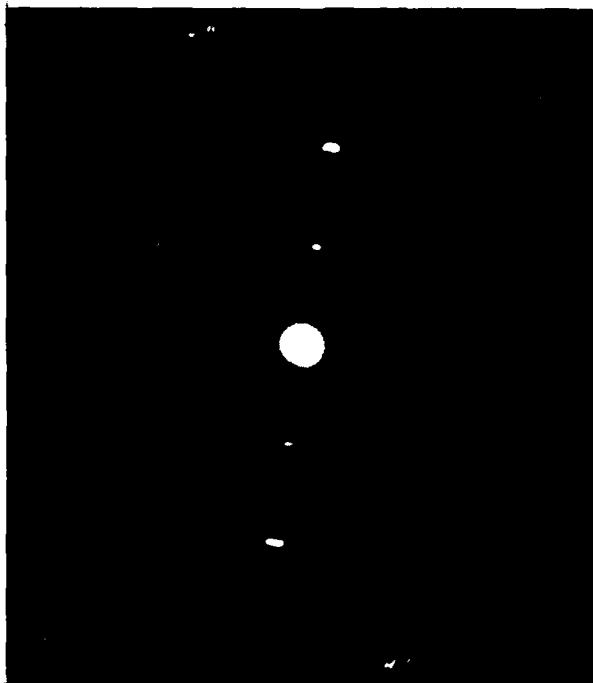


Figure 5. Al-rich martensite phase consisting of alternate twins in the boron-free ribbon.



$M_{23}B_6 - D8_4 (110) \text{ zone}$

Figure 6.  $M_{23}B_6$  boride precipitates developed in the ribbon containing 4.0 at% boron.

**APPENDIX C**





CORPORATE RESEARCH AND DEVELOPMENT • SCHENECTADY, NEW YORK

**BORON SOLUBILITY  
AND STRENGTHENING POTENCY  
IN RAPIDLY SOLIDIFIED  $\text{Ni}_3\text{Al}$**

by  
S.C. Huang, A.I. Taub, and K.M. Chang  
Metallurgy Laboratory

TECHNICAL INFORMATION SERIES

1

CLASS

Report No. 84CRD049

March 1984

GENERAL  ELECTRIC

GENERAL  ELECTRIC

General Electric Company  
Corporate Research and Development  
Schenectady, New York 12345

# TECHNICAL INFORMATION SERIES

<b>AUTHOR</b> Huang, SC Taub, AI Chang, KM	<b>SUBJECT</b> Ni <sub>3</sub> Al-base alloys	<b>NO.</b> 84CRD049
		<b>DATE</b> March 1984
<b>TITLE</b> Boron Solubility and Strengthening Potency in Rapidly Solidified Ni <sub>3</sub> Al		<b>GE CLASS</b> 1
		<b>NO. PAGES</b> 5
<b>ORIGINATING COMPONENT</b> Metallurgy Laboratory		<b>CORPORATE RESEARCH AND DEVELOPMENT</b> SCHENECTADY, N.Y.
<b>SUMMARY</b> <p>The strengthening of the intermetallic compound Ni<sub>3</sub>Al by boron addition has been investigated via the rapid solidification technique of melt spinning. Using X-ray diffraction, differential thermal analysis and transmission electron microscopy it is shown that by rapid solidification up to 1.5 at.% boron can be held in solution in the aluminide without formation of boride. The lattice parameter results further show that the boron atoms in solution tend to occupy the interstitial sites, generate large lattice strain, and thereby strengthen the Ni<sub>3</sub>Al substantially. For example, addition of 1 at.% boron increases the Ni<sub>3</sub>Al room temperature yield strength to ≈750 MPa. This represents a strengthening potency significantly larger than that of substitutional solutes.</p>		
<b>KEY WORDS</b> Ni <sub>3</sub> Al, boron solubility, mechanical behaviors, rapid solidification, interstitial solute		

INFORMATION PREPARED FOR \_\_\_\_\_

Additional Hard or Microfiche Copies  
Available from

Technical Information Exchange  
Bldg. 5 Room 321, Schenectady, N.Y. 12345

# BORON SOLUBILITY AND STRENGTHENING POTENCY IN RAPIDLY SOLIDIFIED $\text{Ni}_3\text{Al}$

S.C. Huang, A.I. Taub, and K.M. Chang

## 1. INTRODUCTION

The alloying behavior of the intermetallic compound  $\text{Ni}_3\text{Al}$  was first studied in detail by Guard and Westbrook.<sup>(1)</sup> It was found that a number of solute elements tended to substitute for either Ni, Al or both, and gave rise to various degrees of solid solution hardening. Those findings on the hardening effect of substitutional solutes subsequently became the basis of investigations aimed at strengthening the aluminide.<sup>(2,3)</sup> Carbon was also studied in Reference 1, but failed to demonstrate the large hardness increase expected from an interstitial solute. Recently, however, remarkable strength increases were observed in rapidly solidified  $\text{Ni}_3\text{Al}$  containing boron,<sup>(4)</sup> which is also an interstitial element. For example, a room temperature yield strength of  $\approx 750$  MPa was measured for a melt-spun  $\text{Ni}_3\text{Al}$  doped with 1.0 at.% boron (compared with  $< 250$  MPa for conventionally treated, pure  $\text{Ni}_3\text{Al}$ ). The contribution of the refined microstructure to the observed strength improvement has been discussed<sup>(4,5)</sup> and other possible strengthening mechanisms such as that of antiphase boundaries<sup>(6)</sup> are being evaluated further. In this paper we report the lattice strain variations and the yield strength increases in melt-spun  $\text{Ni}_3\text{Al}$  ribbons caused by the addition of boron. Complemented by other techniques, the lattice parameter measurements allow the determination of the boron solubility in rapidly solidified  $\text{Ni}_3\text{Al}$ . Further, the lattice strain results provide insight into the solution nature of the boron atoms and explain the observed boron strengthening effect in accordance with Mott and Nabarro's solid solution hardening theory.<sup>(7)</sup>

## 2. EXPERIMENTAL

Ingots of  $(\text{Ni}_{0.75}\text{Al}_{0.25})_{100-x}\text{B}_x$  containing up to 6 at.% boron were prepared by vacuum induction melting using high-purity Ni, Al and NiB. The alloys were then melt spun in vacuum into ribbons approximately 6 mm wide by  $35\text{ }\mu\text{m}$  thick. The ribbon solidification rate is estimated to be greater than  $10\text{ cm/s}$ ,<sup>(8)</sup> which is equivalent to a ribbon cooling rate greater than  $5 \times 10^5\text{ K/s}$ . To determine the lattice parameter, the surfaces of the ribbons were subjected to X-ray diffraction (XRD) in a Siemens D500 diffractometer equipped with a beam monochromator.

$\text{Cu K}\alpha$  radiation was used, which has a specimen penetration depth of  $\approx 10\text{ }\mu\text{m}$ . Also, differential thermal analysis (DTA) and transmission electron microscopy (TEM) were performed to detect and characterize the second phase in the high-boron ribbons. The TEM samples were prepared by jet-electropolishing both of the ribbon surfaces in a solution of two parts perchloric acid (70%) plus eight parts methanol. Finally, the ribbons were tensile tested at room temperature in an Instron machine at a strain rate of  $8.3 \times 10^{-4}\text{ s}^{-1}$ .

## 3. RESULTS

The XRD measurements of the lattice parameter of the rapidly solidified  $\text{Ni}_3\text{Al}$  as a function of boron content are summarized in Figure 1. In this figure, the circles represent the data obtained from the wheel-contacting surface of the ribbons, and the squares are the data from the noncontacting surface. As shown,

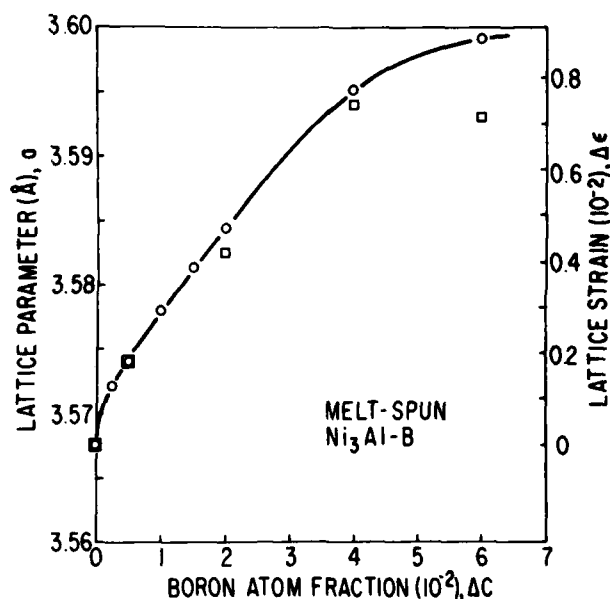


Figure 1. The lattice parameter and the lattice strain as a function of the boron concentration in melt-spun  $\text{Ni}_3\text{Al}$ . O -- measured on the wheel-contacting surface of the ribbons;  $\square$  -- measured on the noncontacting surface of the ribbons.

the lattice parameter increases monotonically with boron concentration, showing no obvious solution limit. At low boron concentrations the lattice parameters measured on the two surfaces of a ribbon agree with each other. At high boron concentrations they differ, suggesting incomplete boron solutioning. In fact, the XRD patterns for ribbons of 4 and 6 at.% boron show a few diffraction lines that are attributable to a second phase, but they are too diffuse for precise phase identification. The DTA measurements also indicate the presence of a second phase at high boron levels. Specifically, DTA measurements of ribbons doped with less than 2.0 at.% boron show only the melting endotherm at  $\approx 1360^\circ\text{C}$ , while the 2.0 at.% boron ribbon exhibits an endothermal peak at  $\approx 1150^\circ\text{C}$  in addition to the melting peak. The low-temperature peak increases in intensity with further increases in boron concentration. It is therefore believed to be due to a low melting  $\text{Ni}_3\text{Al}$ -boride eutectic as reported by Stadelmaier et al.<sup>(9)</sup> As additional evidence, electron diffraction analysis confirms the existence of an  $\text{M}_{23}\text{B}_6$  phase in ribbon containing  $\text{B} > 1.5$  at.%, Figure 2. No boride phase can be found in ribbons containing  $\text{B} \leq 1.5$  at.% (Figure 3).

The mechanical behavior of the  $\text{Ni}_3\text{Al}$ -base ribbons has been studied by tensile tests at room temperature. As reported previously,<sup>(4,5)</sup> the ribbon ductility increases with boron addition (to a maximum fracture strain of  $\approx 10\%$  elongation at 1.0 at.% boron). However, boron additions greater than 1.5 at.% result in ribbon embrittlement, and thus preclude the determination of 0.2% offset yield strength since fracture occurs during elastic loading. The yield strength as a function of boron concentration within the limit of 1.5 at.% is summarized in Figure 4. As shown in this figure, the yield strength of the pure  $\text{Ni}_3\text{Al}$  ribbon is determined to be 480 MPa at room temperature. Fur-

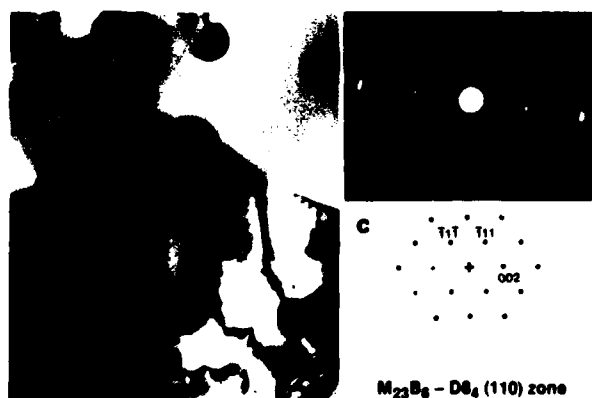


Figure 2. A transmission electron micrograph of the melt spun  $\text{Ni}_3\text{Al}$  ribbon containing 4.0 at.% boron, showing the  $\text{M}_{23}\text{B}_6$  boride precipitates.

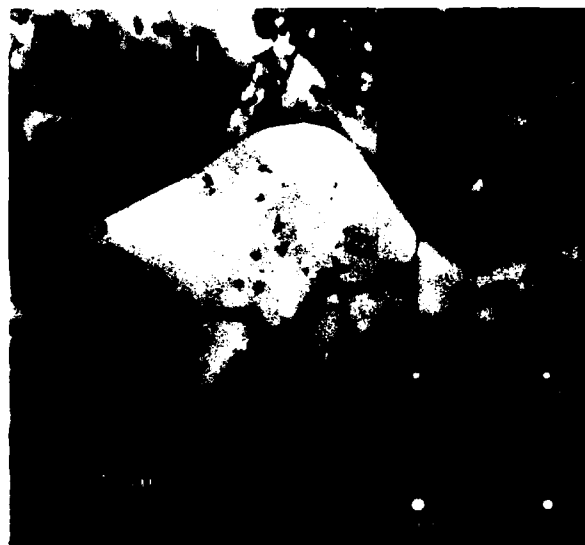


Figure 3. A transmission electron micrograph of the melt-spun, single-phase, ordered  $\text{Ni}_3\text{Al}$  containing 0.5 at.% boron.

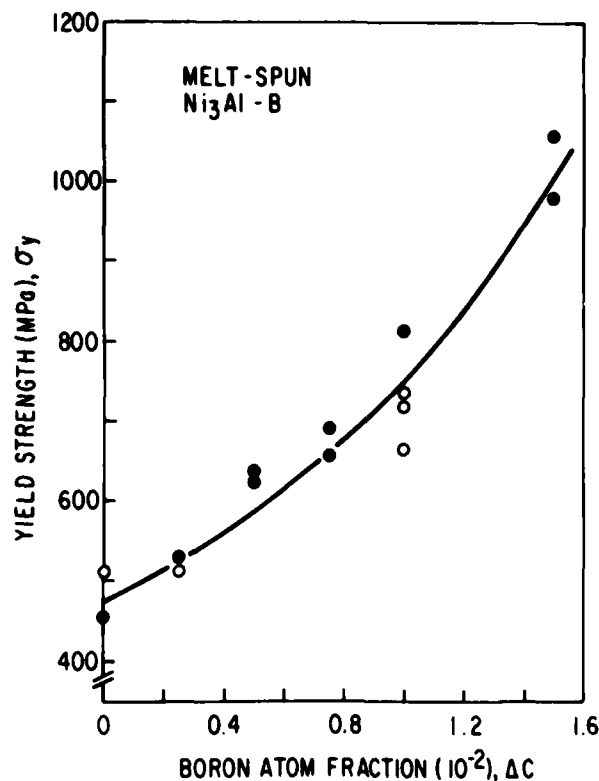


Figure 4. The room temperature yield strength as a function of boron concentration in melt-spun  $\text{Ni}_3\text{Al}$ . The open circles are data from Reference 4. The yield strength for the 0 as well as the 1.5 at.% boron alloy is actually the fracture stress obtained from testing ribbons, since fracture occurs in the elastic region.

ther, the ribbon yield strength is seen to increase nearly linearly with a boron addition, approaching 750 MPa at the boron concentration of 1.0 at. %.

#### 4. DISCUSSION

The equilibrium boron solubility in  $\text{Ni}_3\text{Al}$  has not been previously reported. However, according to a Ni-Al-B ternary phase diagram,<sup>(9)</sup> the boron solubility in  $\text{Ni}_3\text{Al}$  might be regarded as similar to that in Ni, i.e., approximately 0.2 at. %. Recent reports<sup>(10,11)</sup> suggest that up to 0.5 at. % boron can remain in solution in copper-chilled, homogenized  $\text{Ni}_3\text{Al}$ . In comparison, the present XRD, DTA and TEM results indicate a boron solubility that is extended by the rapid solidification technique of melt spinning to at least 1.5 at. %. Within this limit, complete solutioning of boron occurs in melt-spun  $\text{Ni}_3\text{Al}$  without boride formation (Figure 3). However, it should be noted that in Figure 1 the lattice parameter of the  $\text{Ni}_3\text{Al}$  ribbons continues to increase for boron levels beyond 1.5 at. %. It thus appears that supersaturation of boron beyond the full solution limit can occur as a result of rapid solidification, although the boride formation cannot be avoided completely. As seen in a high-boron ribbon in Figure 2, the  $\text{M}_{23}\text{B}_6$  boride is likely to form in regions near the ribbon noncontact surface where the cooling rate is reduced. This is corroborated by the results of Figure 1 which show that lattice parameter and thus the amount of boron saturation is decreased at the noncontact surface of the high-boron ribbons. It should also be noted that in Figure 1 the relationship between the lattice parameter and the boron concentration exhibits a slight nonlinearity, even within the full solution limit of 1.5 at. %. This nonlinearity was not observed in the  $\text{Ni}_3\text{Al}$  solid solutions containing substitutional solutes,<sup>(1)</sup> and it perhaps reflects a tendency for boron atoms to form  $\text{B}_2$  pairs in the configuration of split interstitials or to partition between the interstitial and substitutional sites.

The lattice parameter measured for the melt-spun ribbon of pure  $\text{Ni}_3\text{Al}$  is  $a_0 = 3.5676 \text{ \AA}$ . A comparison with the standard  $\text{Ni}_3\text{Al}$  lattice constant of  $3.561 \text{ \AA}$  suggests that some lattice distortion is induced by residual thermal stress as a result of the rapid solidification melt spinning technique. For the  $\text{Ni}_3\text{Al}$  containing boron, the rapid solidification process also entraps the boron in solution, giving rise to extra lattice distortion. Since the  $\text{Ni}_3\text{Al}$  lattice cell expands as a result of the boron addition (cf. Figure 1), boron atoms seem to prefer the interstitial rather than the substitutional positions. The lattice dilation strain,  $\Delta\epsilon$ , in a boron-doped  $\text{Ni}_3\text{Al}$  ribbon can be calculated from the lattice parameter,  $a$ , using the equation  $\Delta\epsilon = (a - a_0)/a_0$ . The calculated lattice strain shown in Fig-

ure 1 reaches a value of  $3.84 \times 10^{-3}$  at the full boron solubility limit of 1.5 at. %. The average lattice strain per boron atom fraction is thus  $\Delta\epsilon/\Delta C = 0.26$ , which is approximately 10 times that of the substitutional elements such as Ti and Mo,<sup>(1)</sup> providing further evidence of the interstitial nature of the boron.

As shown in Figure 4, the melt-spun  $\text{Ni}_3\text{Al}$  alloys exhibit high strength at room temperature. The yield strength determined for the pure  $\text{Ni}_3\text{Al}$  ribbon ( $\approx 480 \text{ MPa}$ ) is significantly greater than that reported for slowly cooled or heat-treated  $\text{Ni}_3\text{Al}$  ( $< 250 \text{ MPa}$ ).<sup>(12)</sup> Boron addition improves the ribbon yield strength further. From Figure 4, the average yield strength increment per atom fraction of boron addition is on the order of  $\Delta\sigma_y/\Delta C = 0.4 \text{ G}$ , where the  $\text{Ni}_3\text{Al}$  shear modulus  $G$  is  $6.5 \times 10^4 \text{ MPa}$ .<sup>(13)</sup> In comparison, the strengthening potency,  $\Delta\sigma_y/\Delta C$ , of substitutional solutes in  $\text{Ni}_3\text{Al}$  ranges from only  $\approx 0.01 \text{ G}$  for Fe to  $\approx 0.08 \text{ G}$  for Ta.<sup>(2)</sup>

The improvement in the yield strength of the rapidly solidified, pure  $\text{Ni}_3\text{Al}$  ribbon is to a large extent attributed to the quenched-in residual stresses and the refined microstructures, viz., grains with a diameter of  $5\text{--}10 \mu\text{m}$  and subgrain cells of  $0.2\text{--}0.5 \mu\text{m}$ .<sup>(4,5)</sup> The boron additions within the solution limit, however, result in no further microstructural refinements.<sup>(5)</sup> Also, the antiphase domain structure, reported by Inoue et al.<sup>(6)</sup> to be an important strengthening feature in rapidly solidified  $\text{L}_{12}$ -type alloys, has not been observed in the present series of ribbons. As shown in the TEM micrograph of Figure 3, only intragranular dislocations can be seen. Therefore, the large strengthening potency measured for boron in melt-spun  $\text{Ni}_3\text{Al}$  is attributable to the solid solution hardening effect of boron. More specifically, Mott and Nabarro<sup>(7)</sup> have concluded that the strength increase in a solid solution can be accounted for by the lattice strain generated by the solute atoms. According to that model, the solute strengthening potency,  $\Delta\sigma_y/\Delta C$ , can be correlated to the lattice strain per atom fraction of solute,  $\Delta\epsilon/\Delta C$ , as in the following expression:

$$\Delta\sigma_y/\Delta C = 2G(\Delta\epsilon/\Delta C)$$

In Figure 5, the empirical correlation of  $\Delta\sigma_y/\Delta C$  vs.  $\Delta\epsilon/\Delta C$  is shown for the interstitial boron (based on the results of Figures 1 and 4) as well as the substitutional elements of Fe, Cr, V, Ti and Si (which have both  $\Delta\sigma_y/\Delta C$  and  $\Delta\epsilon/\Delta C$  reported in References 1 and 2). As shown in this figure, there exists a linear relationship between  $\Delta\sigma_y/\Delta C$  and  $\Delta\epsilon/\Delta C$ , having a slope of  $\approx 1.6 \text{ G}$  which agrees in general with the Mott and Nabarro theory on the solid solution hardening effect. More interestingly, boron stands out as a particularly potent strengthener in  $\text{Ni}_3\text{Al}$ , due to the large

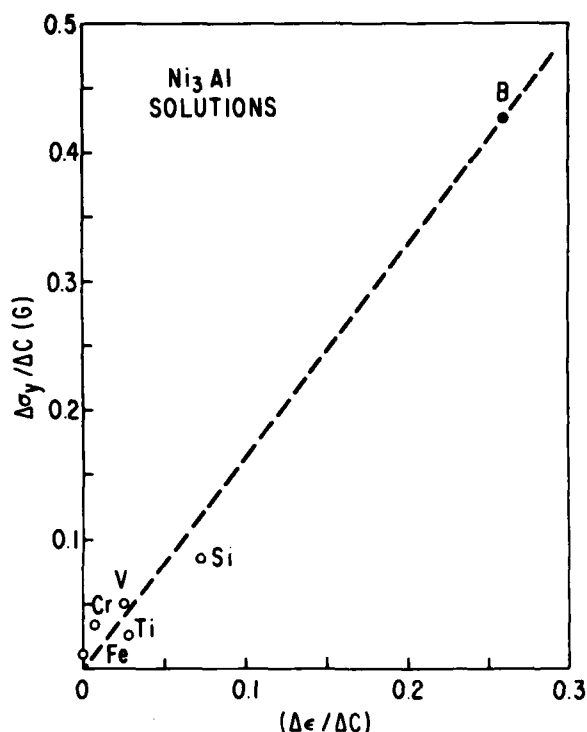


Figure 5. The correlation of strengthening potency,  $\Delta\sigma_y/\Delta C$ , to the lattice strain per solute atom fraction,  $\Delta\epsilon/\Delta C$ , for boron and a variety of other solute elements in  $\text{Ni}_3\text{Al}$ .<sup>(1,2)</sup> The  $\Delta\sigma_y/\Delta C$  values are normalized to the  $\text{Ni}_3\text{Al}$  shear modulus,  $G = 6.5 \times 10^4 \text{ MPa}$ .<sup>(13)</sup>

lattice strain that it produces by occupying the interstitial lattice positions.

The microhardness of rapidly solidified  $\text{Ni}_3\text{Al}$  (24 at.% Al) containing boron of 0, 0.25, and 0.5 at.% has recently been studied by Koch et al.,<sup>(14)</sup> using foils prepared by the arc-hammer technique. The results showed no obvious variations in hardness as a function of boron concentration, contrary to the present results on the boron strengthening effect. The TEM microstructure of those foils consisted of nonuniform antiphase domains in grain interiors and apparent second-phase precipitates at grain or cell boundaries, indicating solute segregation during the foil solidification. Neither of the above foil microstructural features has been observed in melt-spun  $\text{Ni}_3\text{Al}$  ribbons doped with the same amount of boron (see Figure 3). No foil lattice parameter data were reported. The discrepancies in microstructure and boron hardening (strengthening) behavior in ribbons vs. foils are not fully understood at this time, but they might be related to differences in the alloy stoichiometry and rapid solidification conditions, or to the difficulties in obtaining precise hardness measurements in thin-gauge foils.

## 5. CONCLUSIONS

In summary, we have obtained complete boron solubility of up to 1.5 at.% in single phase  $\text{Ni}_3\text{Al}$  by the rapid solidification melt-spinning process. Beyond the limit of full solution, additional boron can still be entrapped in the  $\text{Ni}_3\text{Al}$  matrix, but not without the formation of  $\text{M}_{23}\text{B}_6$  boride. Within the full solution limit, the boron atoms tend to occupy the interstitial sites and produce a large lattice dilation ( $\Delta\epsilon = 0.0026$  per atom percent of boron). As a result, boron becomes an effective strengthener in  $\text{Ni}_3\text{Al}$ , having a strengthening potency of  $\Delta\sigma_y/\Delta C = 0.4\text{G}$ .

## ACKNOWLEDGMENTS

The authors wish to acknowledge R.J. Zabala, R.P. Laforce, L.C. Perocchi, C.P. Palmer, C.I. Hejna, and P.C. Irwin for technical support, and E.L. Hall, C.L. Briant, F.E. Luborsky, M.R. Jackson and L.A. Johnson for helpful discussions. This work is supported in part by the Office of Naval Research under the contract N00014-83-C-0199.

## REFERENCES

1. R.W. Guard and J.H. Westbrook, *Trans. AIME*, 215 (1959) 807.
2. R.D. Rawlings and A.E. Staton-Bevan, *J. Mat. Sci.*, 10 (1975) 505.
3. P.H. Thornton, R.G. Davies and T.L. Johnston, *Met. Trans.*, 1 (1970) 207.
4. A.I. Taub, S.C. Huang and K.M. Chang, to appear in *Met. Trans.*
5. K.M. Chang, S.C. Huang, and A.I. Taub, to be published in *Proc. Symp. Rapidly Solidified Metastable Materials*, The Materials Research Society Meetings, Boston, Nov. 15-17, 1983.
6. A. Inoue, H. Tomiska and T. Masumoto, *Met. Trans. A*, 14 (1983) 1367.
7. N.F. Mott and F.R.N. Nabarro, in "Report on Conference on the Strength of Solids," *Phys. Soc.*, London, 1948, p. 1.
8. S.C. Huang and R.P. Laforce, as in Reference 5.
9. H.H. Stadelmaier and A.C. Fraker, *Metall.*, 16 (1962) 212.
10. K. Aoki and O. Isumi, *J. Japn Inst. Met.*, 43 (1979) 1190.
11. C.T. Liu and C.C. Koch, in "Technical Aspects of Critical Materials Use by the Steel Industry," Vol. IIB, National Bureau of Standards, 1983, p. 42-1.
12. E.M. Grala, in "Mechanical Properties of Intermetallic Compounds," ed. J.H. Westbrook, John Wiley and Sons, NY, 1960, p. 358.
13. K. Ono and R. Stern, *Trans. AIME*, 245 (1969) 171.

14. C.C. Koch, J.A. Horton, C.T. Liu, O.B. Cavin and J.O. Scarbrough, "Rapid Solidification Processing, Principles and Technologies III," ed. R.

Mehrabian, National Bureau of Standards, 1983, p. 264.

END

FILMED

9484

DTIC